Stannoxane capping derived from chiral tridentate NNO donor ligand for nickel and copper macrocycles: Comparative binding studies of stannoxane moiety and its modulated copper comp...

ARTICLE *in* JOURNAL OF ORGANOMETALLIC CHEMISTRY · MAY 2007

Impact Factor: 2.17 · DOI: 10.1016/j.jorganchem.2007.07.044

Available online at www.sciencedirect.com
ScienceDirect
Journal of Organometallic Chemistry 692 (2007) 5156–5164
Journal of Organometallic Chemistry
www.elsevier.com/locate/jorganchem

Stannoxane capping derived from chiral tridentate NNO donor ligand for nickel and copper macrocycles: Comparative binding studies of stannoxane moiety and its modulated copper complex with CTDNA

Mala Chauhan, Farukh Arjmand *

Department of Chemistry, Aligarh Muslim University, Aligarh, Uttar Pradesh 202002, India

Received 11 May 2007; received in revised form 26 July 2007; accepted 27 July 2007
Available online 3 August 2007

Abstract

Novel stannoxane type dinuclear tin complex $C_{16}H_{13}N_4O_2Sn_2Cl_7$ (**1**) and its modulated macrocyclic complexes $[C_{24}H_{36}N_{10}O_3Sn_2CuCl_7]$ ClO_4 (**2**) and $[C_{24}H_{34}N_{10}O_2Sn_2NiCl_7]$ ClO_4 (**3**) were synthesized and characterized by elemental analysis and various spectroscopic techniques (IR, ^1H, ^{13}C, ^{119}Sn NMR, ESI-MS, EPR and UV-Vis). ^{119}Sn NMR shows the presence of two tin metal centers in different environment. The proposed pseudo-octahedral geometry of copper in complex **2** and square pyramidal geometry of nickel in complex **3** were established by the analysis of spectroscopic data. Absorption and fluorescence spectral studies and viscosity measurements have been carried out to assess the comparative binding of dinuclear stannoxane complex **1** and its modulated copper complex **2** with calf thymus DNA. The intrinsic binding constants K_b of the complex **1** and **2** were determined as 4.4×10^4 M^{-1} and 7.5×10^4 M^{-1}, respectively. Cyclic voltammetric studies have also been employed to ascertain the binding of complex **2** with CTDNA. The results suggest that the complex **2** binds to CTDNA twice in the order of magnitude compared to complex **1**. Interaction studies of complex **2** with guanosine 5′-monophosphate further confirm the binding via N_7 position of guanine and phosphate moiety.

Keywords: Stannoxane capping; Binding studies; CT-DNA; 5′GMP; UV-Vis; Fluorescence; Cyclic voltammetry

1. Introduction

Tin and organotin compounds exhibit wide spectrum biological activity [1–5] and are notably important in the discovery of new metal-based anticancer chemotherapeutic agents [6–10]. This class of compounds has gained tremendous impetus because their *in vitro* antitumor activity is greater than *in vivo* activity of cisplatin – a well-known cancer drug especially used for treating testicular, ovarian, bladder and head/neck cancers [10]. The binding ability of organotin compounds towards DNA depends on the coordination number and the nature of group bonded to the central tin atom. The phosphate group of DNA sugar backbone usually acts as an anchoring site and nitrogen of DNA base binding is extremely effective, this often resulting in the stabilization of the tin center as an octahedral stable species [11].

In an attempt to discover a novel metal-based antitumor agent with a different therapeutic profile than cisplatin which failed owing to multiple reasons such as severe toxicity, side effects and resistance, we have employed a new strategy of synthesis involving capping/modulating the transition metal Cu(II)/Ni(II) embedded macrocycle with a biologically significant moiety which is benzimidazole derived –NNO donor tridentate chiral stannoxane. This stannoxane capping creates interesting differences in space

* Corresponding author. Tel.: +91 05712703893.
E-mail address: farukh_arjmand@yahoo.co.in (F. Arjmand).

0022-328X/$ - see front matter © 2007 Elsevier B.V. All rights reserved.
doi:10.1016/j.jorganchem.2007.07.044

configuration and electronic structure, besides inducing chirality in nickel/copper macrocycles, which is further responsible for specific and selective binding affinity at the molecular target site [12,13]. Besides this, tin compounds are known to act as strong apoptotic directors, activate apoptosis directly via p53 tumor suppressor pathway. These complexes bear structural resemblance to the other bimetallic complexes reported earlier by our group [14,15] containing Cu^{II} and Sn^{IV} ions which have demonstrated manifold increase in the binding affinity as well as a dual mode of action due to preferential selectivity of the metal ions inside the cells [16,17]. Herein, we report the synthesis and characterization of tridentate ligand derived dinuclear tin and its modulated copper complex. Comparative binding studies of complexes **1** and **2** with CT DNA were carried out by various spectroscopic techniques viz. absorption titration, fluorescence spectral studies, and viscosity measurements. Interaction studies of complex **2** with guanosine 5′-monophosphate were also carried out which revealed coordinate binding through N7 atom of guanine.

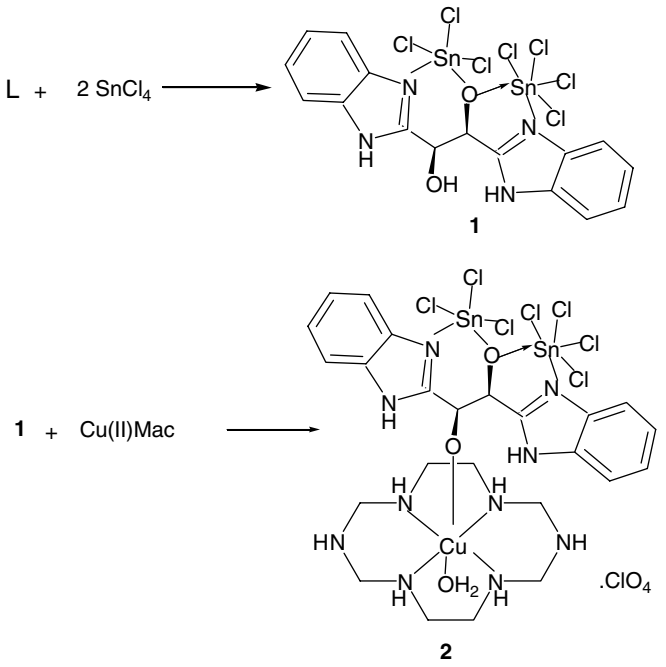

Scheme 1.

2. Results and discussion

Stannoxane type dinuclear complex **1** was synthesized by the reaction of 1,2 Bis (1H-benzimidazol-2yl)-1,2 ethanediol **L** with tintetrachloride. Further, the modulated macrocyclic complexes **2** and **3** were prepared by the reaction of the complex **1** and CuMac and NiMac complexes via second deprotonation, which occurs at pH 10 by the addition of NaOH. The potentiometric titration of ligand reveal that the first deprotonation take place at the alcohol function around 6–8 pH. However, the second deprotonation was not observed below pH 10, which accounts for the stabilization of the second alcohol H atom and probability of H bonding with the anions. These were characterized by various analytical and spectroscopic procedures. ^{119}Sn NMR exhibits the different environment of two tin metal centers. The coordination geometry of central metal ion in complex **2** is octahedral while complex **3** shows square pyramidal geometry around Ni(II) metal ion. Thus, the results are in accordance with the proposed structure (Scheme 1). All the complexes are soluble in DMSO and insoluble in common organic solvent. Complexes **2** and **3** are ionic in nature (1:1 elctrolyte) however, complex **1** is nonelectrolyte. Comparative DNA binding studies were performed with dinuclear Sn complex **1** and modulated macrocyclic copper complex **2**.

2.1. IR spectra

The IR spectra of free ligand **L** displayed ν(OH) bands at 3497 cm^{-1}. A medium intensity band at 1585 cm^{-1} has been assigned to ν(C=N) of imidazole ring and a characteristics ν(N–H) stretching band appeared at 3180 cm^{-1}; ν(C–N) and ν(C–O) appeared at 1317 and 1267 cm^{-1}, respectively. In complex **1**, ν(OH) stretching band disappeared with the emergence of new peak at ca. 3459 cm^{-1} indicating the coordination of the Sn metal ion through the O atom of one of alcohol groups by the elimination of HCl while the other OH remains uncoordinated [18]. The band due to ν(N–H) of the imidazole moiety at 3180 cm^{-1} remains unaltered in all the complexes indicating the nonparticipation of NH group in complex formation [18]. The IR spectra of complex **2** and **3** exhibit absence of ν(OH) band confirming the coordination of OH group of complex **1** to the macrocyclic complex. Furthermore, the ν(C=N) of the imidazole undergoes a negative shift (at 1522 cm^{-1}) indicating the involvement of N atom in the formation of dinuclear tin complex. The ν Sn–O–Sn band appears at ~655 cm^{-1} revealing the presence of stannoxane moiety with three-coordinate oxygen bound to tin atoms. Far IR spectra of the complexes **2** and **3** exhibited absorption at ~433 and ~537 cm^{-1} attributed to ν(M–O) and (M–N) bands, which further confirm the bonding of another O atom of complex **1** to the macrocyclic complexes. All the complexes exhibit (Sn–N) and (Sn–Cl) at ~333 and ~275, respectively, in far IR region [19,20].

2.2. NMR spectra

The ^{1}H NMR spectrum of complex **3** has several interesting features compared to that of free ligand and complex **1**. The ligand **L** revealed OH proton at 5.4 ppm [21]. In complex **1** this peak disappeared, which indicated that the OH group is coordinated to metal center. However, a new signal at 5.9 ppm indicates that one of the OH group is uncoordinated and involved in H-bonding with the anion and solvent [22]. ^{13}C NMR spectrum of complex **1** showed

shift in C–O, carbon atom at 69.4 ppm, which confirm the coordination of O atom of ligand to Sn metal ion. In addition, low field signal at 153.8 observed due to ν(C=N) in comparison to free ligand indicate the coordination of N atom of metal center [23]. ^{119}Sn NMR of complex **1** reveals two signals at 67.8 and 14.2 ppm indicating the presence of two Sn(IV) metal centers in different coordination environments, five- and six-coordinate geometry, respectively in conformity with the proposed structure [24,25].

^{1}H NMR spectrum of complex **3** exhibits the absence of another proton signal at 5.9 ppm confirming the second deprotonation of OH group which occur at pH 10. Other resonances of the complex **3** appeared with slight shift at 4.8, 2.4–3.3, 7.0–7.3 and 8.2 ppm for CH, NH–CH_2–CH_2–NH, aromatic proton and the NH proton of imidazole ring, respectively [26]. ^{13}C NMR spectrum of the complex **3** confirms the ^{1}H NMR data.

2.3. Mass spectroscopy

The complexes have been unambiguously characterized through mass spectral analysis. The electrospray mass spectrum of complex **1** and **2** do not show the molecular ion peak but exhibited other peaks due to the successive fragmentation of the complexes. The mass spectrum of complex **1** showed a prominent peak at *m/z* 295 with a relative abundance of 70% which corresponds to fragment [**1**-$Sn_2Cl_7 + 2H^+$] by the cleavage of the most labile Sn-O bond and a peak at *m/z* 276 (10%) due to [**1**-Sn_2Cl_7OH] fragment. This is further confirmed by the peak occurring at *m/z* 483 (15%) due to [$Sn_2Cl_7 - 2H^+$] fragment. In complex **2** the appearance of peak at *m/z* 813 (20%) is attributed to [**2**-Cl_8O_4]$^+$ ion obtained by the extrusion of Cl^- and ClO_4^- ions. The spectrum of complex **2** also showed peak at *m/z* 816 which can be assigned to [**2**-$SnCl_4H_2O_5 - 2H^+$]$^+$ ion while the peak observed at *m/z* 360 for the fragment [**2**-$C_{16}H_{15}N_4O_3Sn_2Cl_7 - 3H^+$] appears due to the detachment of the stannoxane moiety and water molecule. The above mentioned fragments of complex **1** were also observed in the mass spectrum of complex **2**. These features of the spectra confirm the formation of modulated macrocycles with stannoxane moiety.

2.4. Electronic spectra

The absorption spectra of the complexes were recorded in DMSO, in which they are readily soluble. The electronic spectrum of **2** exhibits a low intensity broad band at 855 nm attributed to a d–d transition, which is typical for pseudo-octahedral environment of copper (II) metal ion [27]. Complex **3** reveal two broad bands at 687 and 407 nm, which have been assigned to $^{3}B(F) \rightarrow {}^{1}E(F)$ and $^{3}B(F) \rightarrow {}^{3}A_2$, $^{3}E(P)$ transitions, respectively [28]. These results are consistent with the pentacoordinate environment around Ni(II) metal ion. All the complexes showed ligand centered intraligand $n \rightarrow \pi^*$ and $\pi \rightarrow \pi^*$ transition at ~274 and ~281 nm, respectively [29].

2.5. EPR spectra

The X-band electron paramagnetic resonance spectrum of copper complex **2** was recorded at a frequency of 9.1 GHz under the magnetic field strength 3000 ± 1000 gauss with tetracyanoethylene (TCNE) as field marker ($g = 2.0027$) at LNT. The complex **2** exhibit an isotropic band centered at $g = 2.14$. This value was in good agreement with an unpaired electron mainly located in dz^2 orbital, typical for octahedral geometry of copper complex [30].

3. DNA binding studies

3.1. Absorption titrations

Electronic absorption spectroscopy is widely employed to determine the DNA binding affinity of metal complexes. Any interaction between the complex and DNA is expected to perturb the ligand centered spectral transitions of the complex. The titration curves were constructed from the fractional changes in absorbance of complexes **1** and **2** as a function of CT DNA concentration. In Uv region, complex **1** and **2** exhibits two absorption bands at 274 and 281 nm assigned to intraligand transitions. Addition of increasing amount of CT DNA to complex **1** resulted in an increase in absorption intensity (hyperchromism of 13.1%) with no shift in wavelength indicating weak binding of the Sn metal ion to the phosphate backbone of the DNA double helix (Fig. 1) [31]. Hyperchromism results from breakage of secondary structure of DNA due to the fact that phosphate group can provide the suitable anchors for coordination in Sn(IV) complexes [1]. In contrast, the complex **2** exhibits hypochromism (15.3%) and also presents a red shift indicative of its coordination through N_7 position of guanine (Figs. 2 and 3). The extent of hypochromism also reveals nature of binding affinity and the hypochromism observed for this complex implies that it

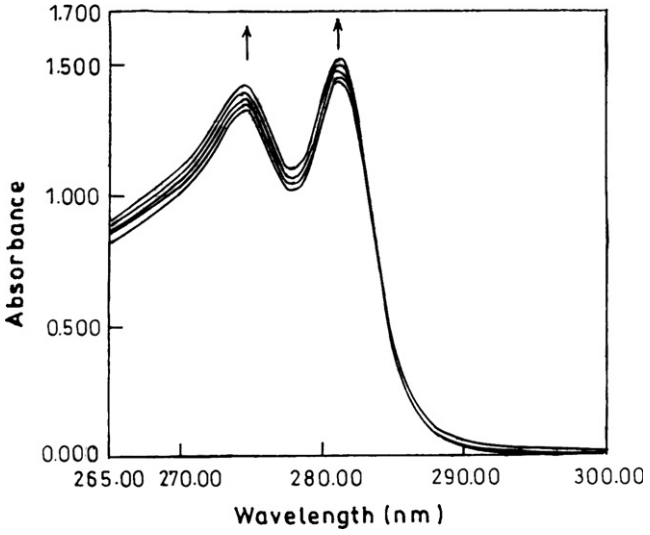

Fig. 1. Absorption spectral traces of complex **1** in Tris–HCl buffer upon addition of CTDNA.

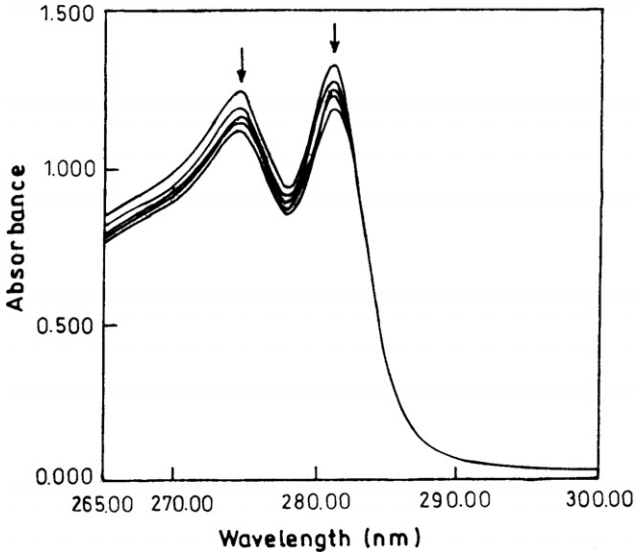

Fig. 2. Absorption spectral traces of complex **2** in Tris–HCl buffer upon addition of CTDNA.

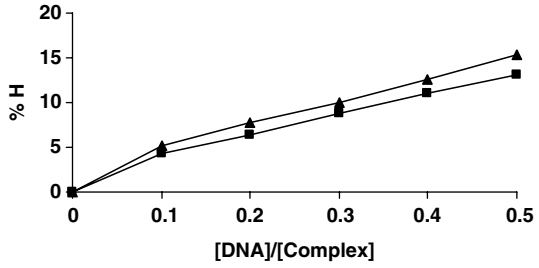

Fig. 3. % Hyperchromism of complex **1** (■) % Hypochromism of complex **2** (▲) upon addition of CTDNA at 274 nm.

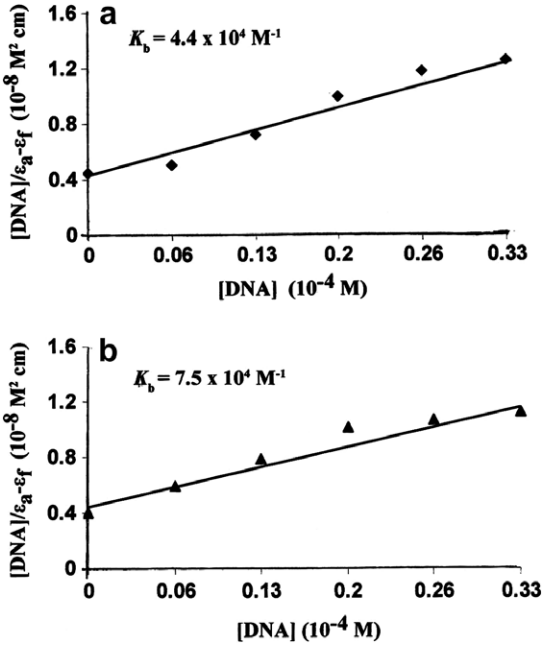

Fig. 4. Plots of $[DNA]/\varepsilon_a - \varepsilon_f$ vs. [DNA] for the titration of CTDNA with (a) complexes **1** (b) complex **2** experimental data points; full lines, linear fitting of the data. $[Complex] = 0.66 \times 10^{-4}$ M, $[DNA] = 0.06–0.33 \times 10^{-4}$ M.

does not intercalate with DNA base pairs. The complex exhibits red shift, which may be decisive for covalent/coordinate linkage mode of binding. To compare the binding strength of complexes quantitatively, the intrinsic binding constants K_b of the complexes **1** and **2** were determined by monitoring the changes of absorbance at 274 nm with increasing concentration of DNA. From the plot of $[DNA]/(\varepsilon_a - \varepsilon_f)$ vs. [DNA], the K_b values of complex **1** and **2** were calculated to be $4.4 \times 10^4\ M^{-1}$ and $7.5 \times 10^4\ M^{-1}$, respectively (Fig. 4). Both of them are much lower than the K_b values of classical intercalators (ethidium bromide) ruling out the possibility of intercalation in the complexes.

Furthermore, these values are closely comparable to some known complexes exhibiting covalent mode of binding [32] and also that K_b value of the complex **2** is two-fold in order of magnitude to complex **1** due to its unique dual reactivity pattern to DNA. Since these complexes possess two metal centers which have preferential selectivity (Copper (II) ion prefers to bind to the N_7 position of guanine while Sn(IV) is selective to the phosphate backbone of the DNA double helix) [33,34]. Therefore, the above results indicate that complex **2** may first bind with the phosphate group of DNA, neutralize the negative charge of DNA phosphate group, and cause the contraction and conformational change of DNA. Investigations of interaction studies of the complex **2** with 5′ GMP provide suitable evidence for such mode of binding.

3.2. Interaction with 5′-GMP

Absorption spectrum of complex **2** which recorded d–d band at 855nm attributed to the pseudo-octahedral environment exhibits distinct spectral changes on interaction with 5′-GMP. These changes give information about the coordination mode as well as additional confirmation of the reaction between nucleotide and complex. On interaction with 5′-GMP, the peak at 855 nm undergoes a gradual decrease (strong hypochromism) followed by emergence of a new peak at 979 nm favoring strong Jahn–Teller distortion. On increasing the concentration of 5′-GMP, there is increase in this absorption peak (Hyperchromism) and a shorter – wavelength isobestic point (i.p.) at 945 nm was recorded revealing dissociation of the proton of the phosphate group. This feature of recording isobestic point practically coincide in Cu^{2+} induced UVD spectrum of the aqueous solution of guanosine and in UVD protonation spectrum of dGMP [35]. Fig. 5 shows that N7 is the coordination site. Moreover, simultaneous interaction with the O6 atom of the phosphate group is likely as in 5′-GMP an amino group and phosphate moiety lie in the same plane. This accounts for coordination mode involving N7 position of guanine [33,36] while hyperchromism of the absorption band at 979 nm reflects further damage caused to

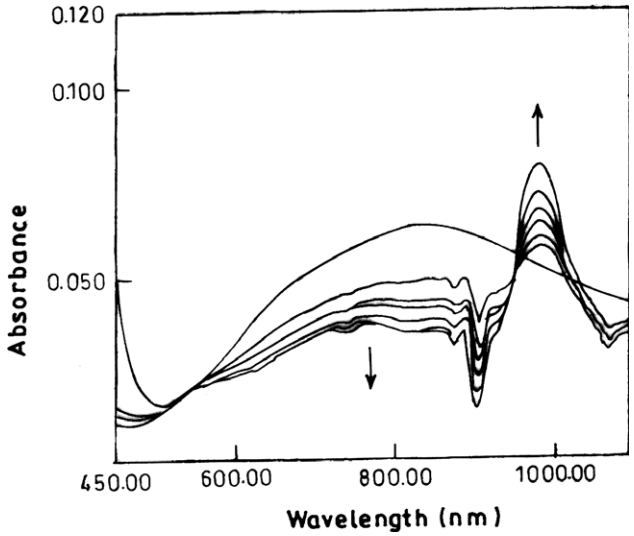

Fig. 5. Absorption spectral traces of complex **2** in DMSO upon addition of 5′-GMP. [Complex **2**] = 1×10^{-4} M, [5′-GMP] = 1–2.6×10^{-5} M.

secondary structure of DNA through phosphate backbone interaction.

3.3. Cyclic voltammetry

Cyclic voltammetry is the most effective and versatile technique available for the mechanistic study of redox systems. The cyclic voltammetric responses of complex **2** in the presence and in the absence of DNA were shown in Fig. 6. Cyclic voltammogram of complex **2** features reduction of +2 to +1 form at a cathodic peak potential $E_{pc} = -0.50$ V and anodic peak potential appeared at $E_{pa} = -0.02$ V. The formal electrode potential E^0 (Voltammetric $E_{1/2}$) taken as the average of E_{pc} and E_{pa} in CV experiments was −0.25 V and $\Delta E_p = 0.50$ V in the absence of DNA. The ratio of anodic to cathodic peak currents is 0.692 suggesting the quasireversiblity of the complex. On addition of CT DNA the peak currents of CV responses of **2** are significantly decreased due to slow diffusion of an equilibrium mixture of the free and DNA bound complexes to the electrode surface [37]. Further, shift in potential $E_{1/2}$ to more negative values indicate the strong binding of complex **2** with CT DNA [38]. Binding studies of complex **1** with CTDNA were not possible as tin complexes are not accessible to the electrode, which causes the peak current of CV waves to diminish greatly.

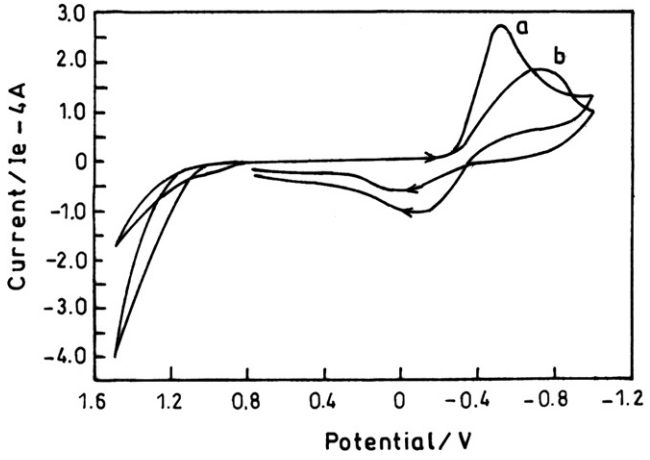

Fig. 6. Cyclic voltammogram (5:95 DMSO/H_2O, 25^0) of (a) unbound complex **2** (b) complex **2** in the presence of CTDNA. [Complex **2**] = 1×10^{-3} M, [DNA] = 6×10^{-3} M.

3.4. Competitive binding studies

No luminescence was observed for complexes **1** and **2** either in DMSO or in the presence of DNA. Hence, competitive binding studies using ethidium bromide bound to DNA was carried out for these complexes. EB emits intense fluorescence in the presence of DNA due to its strong intercalation between the adjacent DNA base pairs. However, the enhanced fluorescence can be quenched evidently when there is a second molecule that can replace the bound EB or break the secondary structure of DNA. The addition of the complex **2** to DNA pretreated with EB causes an appreciable reduction in fluorescence intensity (Fig. 7a). This suggests that the complex **2** competes

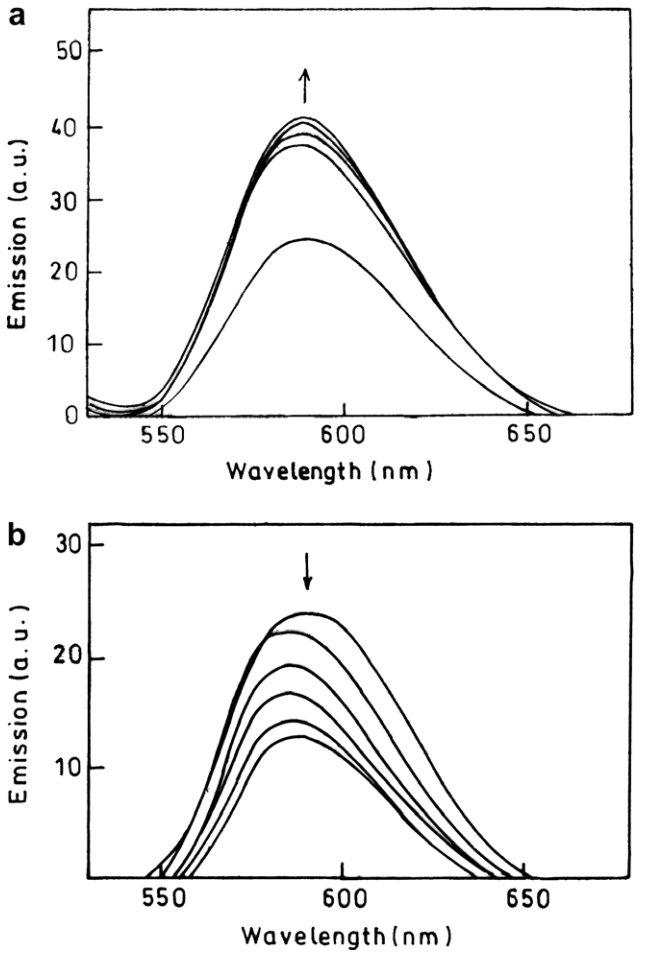

Fig. 7. Emission spectra of EB bound to DNA in the presence of (a) complex **1** (b) complex **2** in Tris–HCl buffer. Arrows shows the intensity changes upon increasing concentration of the complexes.

with EthBr in binding to DNA i.e. the coordination of N_7 atom of guanine to copper metal ion [39]. In contrast to complex **2**, emission intensity of complex **1** increases to a smaller extent (Fig. 7b) [40]. This observed enhancement in emission is only due to the binding of complex to DNA via electrostatic interaction, which involves the binding of tin metal atom to the negatively charged oxygen atom of the phosphate backbone of DNA helix.

The fluorescence quenching curve of EB bound to DNA by the complex **2** is shown in Fig. 8. The quenching curve illustrates that the quenching of EB bound to DNA by the complex is in good agreement with the linear Stern-Volmer equation. In the plot of I_0/I vs. [Cu]/[DNA], K is given by the ratio of the slope to intercept. The K value for complex **2** is 0.20 indicating the strong interaction of complex **2** with CTDNA.

3.5. Viscosity measurements

To further explore the interaction properties between the complexes and the DNA, the specific relative viscosity of DNA was examined by varying the concentrations of added complexes and results are presented in Fig. 9. Photophysical experiments provide necessary but not sufficient clues to support a binding mode. Viscosity measurements is the most critical tests of binding in solution in the absence of crystallographic structure data. Fig. 9 shows the relative changes in viscosity upon addition of complexes **1** and **2**. The relative specific viscosity of CT-DNA decreases with increasing concentration of complexes but decrease for complex **2** is much greater than complex **1** which imply that complex **1** binds to CT-DNA by simple electrostatic binding and complex **2** binds via coordinate covalent mode of interaction [41,42].

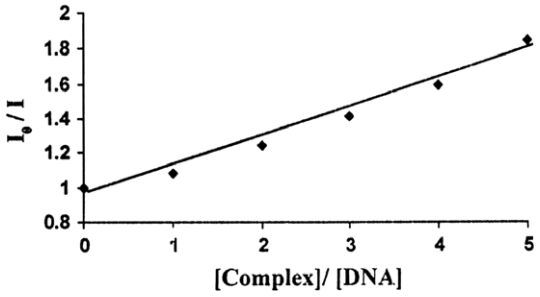

Fig. 8. Fluorescence quenching curve of DNA bound EB by complex **2**. $[EB] = 0.16 \times 10^{-6}$ M, $[DNA] = 3.3 \times 10^{-5}$ M, $[complex] = 16.6 \times 10^{-5}$ M.

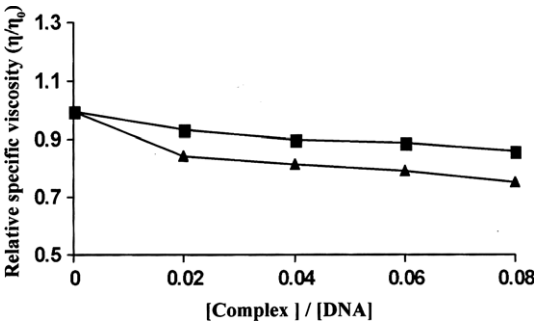

Fig. 9. Effects of increasing amount of complex **1** (■), complex **2** (▲) on the relative viscosity of CTDNA at 29 ± 0.1 °C.

4. Conclusions

We have described the dinuclear stannoxane and its modulated macrocyclic copper/nickel–tin complexes. Isolation of stannoxane complex **1** was a novel finding and it can be utilized as a modulating/tuning agent capable to act as an apoptotic director as well as to restrict the geometry of the macrocycles by coordinatively saturating the molecule. Stannoxane can be used as important chiral precursor in drug design, which can change the course of drug action at the molecular level. The comparative DNA binding studies of stannoxane **1** with complex **2** reveals two-fold increase in the binding strength which is due to the insertion of tin capping and thereby the presence of two metal ions with preferential selectivity. The interaction studies involving complex **2** towards 5′-GMP confirms that DNA binding is governed primarily by a specific interaction between Cu(II) and guanine base at the N7 position while tin appears to interact through the phosphate backbone of DNA double helix. This work underlines some important features for the research on modulated macrocyclic complexes as new anticancer drug and support future evaluation of the compound in cell-based and/or in animal experimental protocols.

5. Experimental

5.1. Materials and measurements

Nickel chloride hexahydrate, copper chloride dihydrate, ethane-1,2-diamine, *tris*-base, L (+) tartaric acid, formaldehyde (E. Merck) Tintetrachloride (Lancaster) and 1,2 diaminobenzene (Loba Chemie) were used as received. Calf thymus DNA (CT-DNA) and guanosine 5′-monophosphate disodium salt (5′-GMP) were purchased from Sigma chemical Co and Fluka, respectively. All reagents grade compounds were used without further purification.

Carbon, hydrogen and nitrogen contents were determined using Carlo Erba Analyzer Model 1106. Molar conductances were measured at room temperature on a Digsun Electronic conductivity Bridge. Fourier-transform IR (FTIR) spectra were recorded on an Interspec 2020 FT-IR spectrometer. UV-Vis spectra were recorded on a UV-1700 PharmaSpec Shimadzu spectrophotometer in DMSO and the data were reported as λ_{max}/nm. The EPR spectrum of the copper complex was acquired on a Varian E 112 spectrometer using X-band frequency (9.1 GHz) at liquid nitrogen temperature in solid state. The ^{1}H and ^{13}C NMR spectra were obtained on a Bruker DRX-300 spectrometer and ^{119}Sn NMR was recorded on a VXR-300 Varian spectrometer operating at room temperature.

Electrospray mass spectra were recorded on Micromass Quattro II.

5.2. DNA binding experiments

All the experiments involving interaction of the complexes with CT DNA were conducted in buffer containing tris(hydroxymethyl)aminomethane (0.01 M) and adjusted to pH 7.5 with hydrochloric acid. The CT DNA was dissolved in Tris–HCl buffer and was dialyzed against the same buffer overnight. Solutions of CT DNA gave ratios of UV absorbance at 260 and 280 nm above 1.8, indicating that the DNA was sufficiently free of protein [43]. DNA concentration per nucleotide was determined by absorption spectroscopy using the molar absorption coefficient 6600 $dm^3\ mol^{-1}\ cm^{-1}$ at 260 nm [44]. Concentrated stock solutions of the complexes were prepared by dissolving the complex **1** and **2** in DMSO and diluting suitably with the corresponding buffer to the required concentrations for all the experiments. Solution of 5′-GMP was prepared in double distilled water.

5.2.1. Absorption spectral experiments

Absorption spectral titration experiments were performed on USB 2000 Ocean Optics spectrophotometer. Maintaining a constant concentration of the complexes (0.66×10^{-4} M) while varying the nucleic acid concentration (0-0.33×10^{-4} M). This was achieved by dissolving an appropriate amount of the metal complex and DNA stock solutions while maintaining the total volume constant. This result in a series of solutions with varying concentrations of DNA but with a constant concentration of the complexes. The absorbance (A) of the most shifted band of investigated complexes were recorded after successive additions of CT DNA. A reference cell contained DNA alone to nullify the absorbance due to the DNA at the measured wavelength. From the absorption titration data, the intrinsic binding constant (K_b) of the copper (II) complex with CT DNA was determined using the equation,

$$\frac{[DNA]}{\varepsilon_a - \varepsilon_f} = \frac{[DNA]}{\varepsilon_b - \varepsilon_f} + \frac{1}{K_b(\varepsilon_b - \varepsilon_f)} \quad (1)$$

where ε_a, ε_f and ε_b correspond to A_{obsd}/[Complex], the extinction coefficient for free copper complex, and the extinction coefficient for the complexes in the fully bound form, respectively. A plot of [DNA]/($\varepsilon_a - \varepsilon_f$) vs. [DNA], where [DNA] is the concentration of DNA in the base pairs, gives K_b as the ratio of slope to the intercept [45].

5.2.2. Luminescence experiments

Emission intensity measurements were carried out using Hitachi F-2500 fluorescence spectrophotometer at room temperature. The tris buffer was used as a blank to make preliminary adjustments. Luminescence titration quenching experiments were conducted by adding aliquots of 3.3–16.6×10^{-5} M solutions of the metal complexes and 3.3×10^{-5} M CT DNA in Tris–HCl buffer. The *Stern-Volmer* equation [46]

$$I_0/I = 1 + K_{sv} r_{Cu} \quad (2)$$

Where I_0 and I are the emission intensities in the absence and the presence of the complex, respectively. K_{sv} is a linear *Stern-Volmer* quenching constant and r_{Cu} is the ratio of total concentration of complex to that of DNA.

5.2.3. Viscosity experiments

Viscosity measurements were carried out from observed flow time of DNA containing solution ($t > 100$ s) corrected for the flow time of buffer alone (t_0), using Ostwald's viscometer at 29 ± 0.01 °C. Flow time was measured with a digital stopwatch. Each sample was measured three times and an average flow time was calculated. Data were presented as (η/η_0) vs. binding ratio ([complex]/[DNA]), [47] where η is a viscosity of DNA in the presence of complex and η_0 is the viscosity of DNA alone. Viscosity values were calculated from the $\eta = t - t_0$ [48].

5.2.4. Cyclic voltammetric experiments

Cyclic voltammetric studies were performed on a CH Instrument Electrochemical analyzer in a single compartmental cell with 0.4 M KNO_3 as supporting electrolyte. A three-electrode configuration was used comprising of a Pt wire as auxiliary electrode, platinum micro cylinder as working electrode and Ag/AgCl as the reference electrode. Electrochemical measurements were made under a dinitrogen atmosphere. All electrochemical data were collected at 298 K and are uncorrected for junctions potentials. The formal potentials, E^0 (or voltammetric $E_{1/2}$) were taken as the average of the anodic (E_{pa}) and cathodic peak potentials (E_{pc}) obtained from cyclic voltammetry.

5.3. Syntheses

5.3.1. 1,2 Bis (1H-benzimidazol-2yl)-1,2 ethanediol (**L**)

The ligand **L** was synthesized with 1,2 diaminobenzene (4.6 g, 40 mmol) and L (+) tartaric acid (3.0 g, 20 mmol) according to the procedure reported earlier [22].

5.3.2. 1,8-Dihydro-1,3,6,8,10,13-hexaazacyclotetradecane copper (II)/nickel(II) diperchlorate (***Cu*/*Ni Mac***)

These complexes were prepared by the following procedure reported by Suh and Kang [49].

To a stirred methanol solution (50 ml) of $CuCl_2 \cdot 2H_2O$ (1.7 g, 10 mmol)/nickel chloride hexahydrate (2.37 g, 10 mmol) were slowly added ethane-1,2-diamine (1.34 ml, 20 mmol), 37% formaldehyde (3.0 ml, 40 mmol) and 25% ammonia (1.0 ml, 20 mmol). The resulting mixture was refluxed for *ca.* 24 h until a dark blue solution appeared. This solution was cooled at room temperature and filtered under vacuum. Excess perchloric acid in methanol was added to the filtrate and the mixture was kept in refrigerator for 24 h. The purple-red crystals for copper and yellow crystals for nickel complexes were separated, washed

thoroughly with methanol, dried *in vacuo* and recrystallized from acetonitrile.

5.3.3. $C_{16}H_{13}N_4O_2\ Sn_2Cl_7$ (**1**)

Tintetrachloride (2.34 ml, 20 mmol) in 6 ml of carbontetrachloride was added to stirred solution of ligand L (2.94 g, 10 mmol) dissolved in methanol. The mixture was stirred for 3 h and left for slow evaporation for 2 days. Cream solid was obtained which was filtered, washed with hexane and dried in vacuo. Yield, 62%, m.p. 258 °C. Anal. Calc. for $C_{16}H_{13}N_4O_2Sn_2Cl_7$(%): C, 24.69; H, 1.68; N, 7.19. Found: C, 24.60; H, 1.65; N, 7.15%. IR (KBr, cm^{-1}) 3459 *ν*(OH), 1522 *ν*(C=N), 1328 *ν*(C–N), 1250 *ν*(C–O), 787 (Ar), 655 *ν*(Sn–O), 333 *ν*(Sn–N), 275 *ν*(Sn–Cl), Uv (DMSO, nm): 274, 281 ^{1}H NMR (DMSO-d_6, ppm): 5.9 (O–H), 7.5–7.8 (ArH), 4.9, 3.4 (inequivalent C–H), ^{13}C NMR (dmso d_6, ppm): 69.4 (C–O), 153.8 (C=N), 115–133 (ArC), (^{119}Sn NMR, DMSO-d_6, ppm): 67.8, 14.8.

5.4. Syntheses of new modulated macrocycles

5.4.1. $[C_{24}H_{36}N_{10}O_3Sn_2\ CuCl_7]\ ClO_4$ (**2**)

A solution of CuMac (0.465 g, 1 mmol) in 50 ml acetonitrile was treated with methanolic solution of $C_{16}H_{13}N_4O_2Sn_2Cl_7$ **1** (0.778 g, 1 mmol). The pH of the reaction mixture was adjusted 10 by adding NaOH solution. The resulting green solution was heated at reflux for 2 h. The solution was then cooled and reduced to 10 ml. Green amorphous solid compound was precipitated which was filtered off washed with a small volume of methanol and dried in vacuo. Yield, 60%, m.p. Anal. Calc. for $[C_{24}H_{36}N_{10}O_3Sn_2CuCl_7]\ ClO_4$ (%): C, 24.84; H, 3.12; N, 12.07. Found: C, 24.80; H, 3.10; N, 12.10%. IR (KBr, cm^{-1}) 1525 *ν*(C=N), 1320 *ν*(C–N), 1221 *ν*(C–O), 787 (Ar), 1081, 620 (ClO_4), 650 *ν*(Sn–O), 330 *ν*(Sn–N), 270 *ν*(Sn–Cl), 433 *ν*(Cu–O), 538 *ν*(Cu–N), UV-Vis (DMSO, nm) 274, 281, 855.

5.4.2. $[C_{24}H_{34}N_{10}O_2Sn_2\ NiCl_7]\ ClO_4$ (**3**)

This complex was synthesized with NiMac (0.460 g, 1 mmol) according to the method outlined above.

Yield, 58%, m.p. Anal. Calc. for $[C_{24}H_{34}N_{10}O_2Sn_2NiCl_7]\ ClO_4$ (%): C, 25.34; H, 3.18; N, 12.31. Found: C, 25.32; H, 3.15; N, 12.30%. IR (KBr, cm^{-1}) 1522 *ν*(C=N), 1322 *ν*(C–N), 1220 *ν*(C–O), 785 (Ar), 1076, 625 (ClO_4), 651 *ν*(Sn–O), 331 *ν*(Sn–N), 269 *ν*(Sn–Cl), 432 *ν*(Ni–O), 535 *ν*(Ni–N), UV–Vis. (DMSO, nm) 277, 285, 407, 687, ^{1}H NMR (DMSO-d_6, ppm): 7.0–7.3 (ArH), 4.8 (C–H), 2.4–3.3 (NH–CH_2–CH_2–NH), 8.2 (NH imidazole), ^{13}C NMR (DMSO-d_6, ppm): 70 (C–O), 153.8 (C=N), 114–132 (ArC).

Acknowledgements

We express our gratitude to Council of Scientific and Industrial Research, New Delhi, for generous financial support (Scheme No. 01 (1982)/05-EMR-II). Thanks to RSIC, CDRI Lucknow for providing CHN analysis data and NMR, and IIT Bombay for EPR measurements. The authors gratefully acknowledge Prof. Sartaj Tabassum, Department of Chemistry, Aligarh Muslim University, Aligarh for providing cyclic voltammetry facility. The authors are extremely thankful to Prof. Claudio Pettinari, Department of Chemistry, University di Camerino, Italy for ^{119}Sn NMR.

References

[1] L. Pellerito, L. Nagy, Coord. Chem. Rev. 224 (2002) 111.
[2] V. Sharma, R.K. Sharma, R. Bohra, R. Ratnani, V.K. Jain, J.E. Drake, M.B. Horsthouse, M.E. Light, J. Organomet. Chem. 651 (2002) 98.
[3] S. Chakraborty, A.K. Bera, S. Bhattacharya, S. Ghosh, A.K. Pal, S. Ghosh, A. Benerjee, J. Organomet. Chem. 645 (2002) 33.
[4] Y. Nath, S. Pokharia, R. Yadav, Coord. Chem. Rev. 215 (2000) 99.
[5] S.J. Casas, A. Castineiras, F. Condori, D.M. Couce, R. Umberto, A. Sanchez, J. Sordo, M.J. Varela, L.M.V. Ezequiel, J. Organomet. Chem. 689 (2004) 620.
[6] T.S.B. Baul, C. Masharing, S. Basu, E. Rivarola, M. Holcapek, R. Jirasko, A. Lycka, D. deVos, A. Linden, J. Organomet. Chem. 691 (2006) 952.
[7] M. Gielen, E.R.T. Tiekink, in: M. Gielen, E.R.T. Tiekink (Eds.), Metallotherapeutic Drug and Metal-based Diagnostic Agents: ^{50}Sn Tin Compounds and Their Therapeutic Potential, Wiley, New York, 2005, pp. 421–439 (Chapter 22).
[8] D.S. Zuo, T. Jiang, H.S. Guan, K.Q. Wang, X. Qi, Z. Shi, Molecules 6 (2001) 647.
[9] A. Chaudhary, A.K. Sing, R.V. Singh, J. Inorg. Biochem. 100 (2006) 1632.
[10] J.J. Bonire, S.P. Fricker, J. Inorg. Biochem. 83 (2001) 217.
[11] S. Tabassum, C. Pettinari, J. Organomet. Chem. 691 (2006) 1761.
[12] S. Shi, J. Liu, J. Li, K.C. Zhang, C.P. Tan, L.M. Chen, L.N. Ji, Dalton Trans. (2005) 2038.
[13] S. Tabassum, S. Parveen, F. Arjmand, Acta Biomater. 1 (2005) 677.
[14] M. Chauhan, F. Arjmand, Trans. Met. Chem. 30 (2005) 481.
[15] M. Chauhan, K. Banerjee, F. Arjmand, Inorg. Chem. 30 (2007) 3072.
[16] N. Hoti, D. Zhu, Z. Song, Z. Wu, S. Tabassum, M. Wu, J. Pharmacol. Exp. Ther. 311 (2004) 22.
[17] N. Hoti, J. Ma, S. Tabassum, Y. Wang, M. Wu, J. Biochem. 134 (2003) 521.
[18] G.F. de Sousa, V.M. Deflon, M.T.P. Gambardella, R.H.P. Francisco, J.D. Ardisson, E. Niquet, Inorg. Chem. 45 (2006) 4518.
[19] M. Pellei, G.G. Lobbia, M. Mancini, R. Spagna, C. Santini, J. Organomet. Chem. 691 (2006) 1615.
[20] C. Ma, Q. Jiang, R. Zhang, Can. J. Chem. 82 (2004) 608.
[21] C. Cativiela, L.R. Falvello, J.C. Gines, R. Navarro, E.P. Urriolabeitia, New J. Chem. 25 (2001) 344.
[22] K. Isele, V. Broughton, C.J. Matthews, A.F. Williams, G. Bernardinelli, P. Franz, S. Decurtins, J. Chem. Soc., Dalton Trans. 20 (2002) 3899.
[23] L. Tei, A.J. Blake, A. Bencini, B. Valtancoli, C. Wilson, M. Schroder, Dalton Trans. (2000) 4122.
[24] A.G. Hernan, P.N. Horton, M.B. Hursthouse, J.D. Kilburn, J. Organomet. Chem. 691 (2006) 1466.
[25] M.N. Xanthopoulou, S.K. Hadjiikakou, N. Hadjiliadis, M. Kubicki, S. Skoulika, T. Bakas, M. Baril, L.S. Butler, Inorg. Chem. 46 (2007) 1187.
[26] Y. Dong, L.F. Lindoy, P. Turner, G. Wei, Dalton Trans. (2004) 1264.
[27] E.W. Ainscough, A.M. Brodie, M. Moubaraki, K.S. Murray, C.A. Otter, Dalton Trans. (2005) 3337.
[28] M.D. Santana, G. Garcia, A. Rufete, M.C.R. De Arellano, G. Lopez, J. Chem. Soc., Dalton Trans. (2000) 619.

[29] F. Arjmand, M. Chauhan, Helv. Chim. Acta 88 (2005) 2413.
[30] V. Chandrasekhar, B.M. Pandian, R. Azhakar, Inorg. Chem. 45 (2006) 3510.
[31] A. Janeso, L. Nagy, E. Moldrheim, E. Sletten, J. Chem. Soc., Dalton Trans. (1999) 1587.
[32] S. Ghosh, A.C. Barve, A.A. Kumbhar, A.S. Kumbhar, V.G. Puranik, P.A. Dater, U.B. Sonawane, R.R. Joshi, J. Inorg. Biochem. 100 (2006) 331.
[33] T. Hirohama, Y. Karunuki, E. Ebina, T. Suzaki, H. Arii, M. Chikira, P.T. Selvi, M. Palaniandavar, J. Inorg. Biochem. 99 (2005) 1205.
[34] T. Ito, S. Thyagarajan, K.D. Karlin, S.E. Rokita, Chem. Commun. (2005) 4812.
[35] V.A. Sorokin, V.A. Valeen, G.O. Gladchenko, I.V. Sysa, Y.P. Blagoi, I.V. Volchok, J. Inorg. Biochem. 63 (1996) 79.
[36] A. Raja, V. Rajendiran, P.U. Maheswari, R. Balamurugan, C.A. Kilner, M.A. Halcrow, M. Palaniandavar, J. Inorg. Biochem. 99 (2005) 1717.
[37] J. Liu, T. Zhang, T. Lu, L. Qu, H. Zhou, Q. Zhang, L. Ji, J. Inorg. Biochem. 91 (2002) 269.
[38] Z.S. Yang, Y.L. Wang, Y.C. Liu, G.C. Zhao, Anal. Sci. 21 (2005) 1355.
[39] Q.Q. Zhang, F. Zhang, W.G. Wang, X.L. Wang, J. Inorg. Biochem. 100 (2006) 1344.
[40] J. Kang, H. Wu, X. Lu, Y. Wang, L. Zhou, Spectrochim. Acta A 61 (2005) 2041.
[41] P.U. Maheswari, M. Palaniandavar, J. Inorg. Biochem. 98 (2004) 219.
[42] S. Tabassum, S. Mathur, J. Carbohy. Chem. 24 (2005) 865.
[43] J. Marmur, J. Mol. Biol. 3 (1961) 208.
[44] M.E. Reicmann, S.A. Rice, C.A. Thomas, P. Doty, J. Am. Chem. Soc. 76 (1954) 3047.
[45] A. Wolfe, G.H. Shimer, T. Meehan, Biochemistry 26 (1987) 6392.
[46] J.R. Lakowiez, G. Webber, Biochemistry 12 (1973) 4161.
[47] G. Cohen, H. Eisenberg, Biopolymers 8 (1969) 45.
[48] M. Eriksson, M. Leijon, C. Hiort, B. Norden, A. Graslund, Biochemistry 33 (1994) 5031.
[49] M.P. Suh, S.G. Kang, Inorg. Chem. 27 (1988) 2544.